

Variational methods for selective mass scaling

Anton Tkachuk · Manfred Bischoff

Received: 26 August 2012 / Accepted: 6 January 2013 / Published online: 23 January 2013
© Springer-Verlag Berlin Heidelberg 2013

Abstract A new variational method for selective mass scaling is proposed. It is based on a new penalized Hamilton's principle where relations between variables for displacement, velocity and momentum are imposed via a penalty method. Independent spatial discretization of the variables along with a local static condensation for velocity and momentum yields a parametric family of consistent mass matrices. In this framework new mass matrices with desired properties can be constructed. It is demonstrated how usage of these non-diagonal mass matrices decreases the maximum frequency of the discretized system and allows for larger steps in explicit time integration. At the same time the lowest eigenfrequencies in the range of interest and global structural response are not significantly changed. Results of numerical experiments for two-dimensional and three-dimensional problems are discussed.

Keywords Selective mass scaling · Variational principle · Dynamics · Hybrid-mixed · Penalty methods

1 Introduction

The basic idea of selective mass scaling (SMS) in the context of non-linear structural dynamics is to add artificial terms to the mass matrix, thus reducing the highest discretized eigenfrequencies of the structure, while changing the lower frequencies as little as possible [1]. SMS aims at reduction of the computational cost, since the highest eigenfrequency of the system limits the critical time step for explicit time inte-

gration. In general SMS can be written in the form

$$\mathbf{M}^\circ = \mathbf{M} + \lambda^\circ, \quad (1)$$

where \mathbf{M}° is the scaled mass matrix, \mathbf{M} is the consistent mass matrix (CMM) or lumped mass matrix (LMM) and λ° is the artificially added mass.

Several methods for SMS are proposed in the literature. Acceleration filtering for thin walled structures modeled with solid elements is suggested in [2]. This approach suppresses relative oscillation in thickness direction via adding inertia for these modes. Two general methods for SMS are given in continuation of that work in [3]. In the first method inertia proportional to the stiffness matrix is added. This method preserves the eigenmodes of the system and the reduction of the highest eigenfrequency can be easily estimated. However, this method is not well suited for non-linear problems where the stiffness matrix changes under large rotations and deformations. The second method uses an algebraically built λ° which does not change upon deformation and rotations. This λ° also preserves translational mass of individual elements. The latter method is easy implementable and it is available in commercial codes, e.g. *LS-DYNA* and *RADIOSS*. However, this method changes eigenmodes and increases rotational inertia of elements. Another motivation of stiffness proportional SMS is given in [4]. It is based on Mindlin's theory of elasticity with micro-inertia, i.e. various strain rate gradients also have inertia. In a recent work [5] an algebraic SMS for thickness direction of solid-shells is proposed. Therein, applicability of SMS for slightly distorted elements was discussed for the first time.

A common disadvantage of all these methods is lack of rigorous formulation and consistency proofs. Moreover, the factor defining the amount of SMS has no clear meaning.

The principal idea of this work is to derive λ° using variational methods. Applying parametrized variational principles

A. Tkachuk (✉) · M. Bischoff
Institut für Baustatik und Baudynamik, Universität Stuttgart,
Pfaffenwaldring 7, 70550 Stuttgart, Germany
e-mail: tkachuk@ibb.uni-stuttgart.de

established in [6] for inertia terms we obtain a new penalized Hamilton’s principle for dynamics. Discretization of the latter principle yields SMS methods with desired properties.

2 Problem statement

Let $\mathcal{B} \subset \mathbb{R}^{\dim}$ be a reference configuration of a body ($\dim = \{1, 2, 3\}$). $\partial\mathcal{B}_u$ and $\partial\mathcal{B}_\sigma$ refer to parts of the body surface where displacement and traction boundary conditions are applied, respectively. Consider the following elasto-dynamic problem for time interval $I = [0, t_{end}]$

$$\begin{cases} \rho \ddot{\mathbf{u}} = \text{div} \boldsymbol{\sigma}(\mathbf{u}) + \hat{\mathbf{b}} & \text{in } I \times \mathcal{B} \\ \mathbf{u} = \mathbf{0} & \text{in } I \times \partial\mathcal{B}_u \\ \boldsymbol{\sigma} \mathbf{n} = \hat{\mathbf{t}} & \text{in } I \times \partial\mathcal{B}_\sigma \\ \mathbf{u}(0, \cdot) = \mathbf{u}_0 & \text{in } \mathcal{B} \\ \dot{\mathbf{u}}(0, \cdot) = \mathbf{v}_0 & \text{in } \mathcal{B} \end{cases} \quad (2)$$

where $\mathbf{u}(t, \mathbf{x}) : \mathbb{R}^{\dim+1} \rightarrow \mathbb{R}^{\dim}$ is the displacement vector, ρ is the density, $\hat{\mathbf{b}}$ and $\hat{\mathbf{t}}$ are the body force and boundary tractions, respectively, \mathbf{u}_0 and \mathbf{v}_0 are initial displacement and velocities. We restrict ourselves to linear constitutive equation given by Hooke’s law

$$\boldsymbol{\sigma} = \mathbf{D} \boldsymbol{\varepsilon}, \quad \boldsymbol{\varepsilon} = \text{sym grad } \mathbf{u} \quad \text{in } \mathcal{B}, \quad (3)$$

with \mathbf{D} , $\boldsymbol{\sigma}$ and $\boldsymbol{\varepsilon}$ being elasticity modulus, stress tensor and engineering strain, respectively.

Equations (2–3) define an initial boundary value problem (IBVP) for an elasto-dynamic problem. An extension to non-linear case is straightforward and it is not discussed herein.

Now we pose a problem to setup a framework which allows a parametric family of *consistent* mass matrices. Such framework should include two parts: an alternative variational principle for dynamics and a discretization procedure.

The following considerations are used for derivation of the new principle. In order to get maximum flexibility for discretization, a multi-field approach with independent variables for displacement, velocity and momentum is used. The fields are linked in a weak sense using the penalty method. The penalty factors then naturally define scaling parameters for the family of mass matrices. Finally, only symmetric terms for inertia should enter the principle, which guarantees symmetric mass matrices by design.

The discretization procedure must be consistent and efficient. Consistency requires at least preservation of translational inertia for a single finite element. Efficiency implies substantial reduction of the highest eigenfrequency that limits the critical time step of the explicit time integration. At the same time lowest eigenfrequencies that define the structural response should not be strongly affected. Moreover, the discretization scheme should not introduce new variables on global level and conditioning of the mass matrix should be

small enough to allow a cheap iterative solution $\ddot{\mathbf{u}} = \mathbf{M}^{-1} \mathbf{f}$. This can be achieved by proper choice of ansatz spaces and parameters of the principle.

3 An alternative variational formulation of dynamic problem

The starting point for derivation of the alternative formulation is Hamilton’s principle [7, Appendix I]. Then, independent variables for velocity and momentum are introduced to the functional. The penalty method is used to link displacement, velocity and momentum in a weak sense. This gives a rise to a parametrized Hamilton’s principle, where kinetic energy is computed on the combination of displacement, velocity and momentum.

The first variation of the principle may be used then as a starting point of discretization. In addition, equivalence of a new principle to the IBVP (2–3) is shown via Euler-Lagrange equations.

Let us introduce notations for a scalar product in the domain, the bilinear forms of potential and kinetic energy and the linear form for external work, respectively

$$(\mathbf{w}, \mathbf{z}) = \int_{\mathcal{B}} \mathbf{w} \cdot \mathbf{z} \, d\mathcal{B}, \quad w, z \in L^2(\mathcal{B}), \quad (4a)$$

$$\Pi^{int}(\mathbf{u}) = \frac{1}{2} a(\mathbf{u}, \mathbf{u}) = \frac{1}{2} \int_{\mathcal{B}} \boldsymbol{\varepsilon}(\mathbf{u}) \cdot \mathbf{D} \boldsymbol{\varepsilon}(\mathbf{u}) \, d\mathcal{B}, \quad (4b)$$

$$T(\dot{\mathbf{u}}) = \frac{1}{2} (\rho \dot{\mathbf{u}}, \dot{\mathbf{u}}) = \frac{1}{2} \int_{\mathcal{B}} \rho \dot{\mathbf{u}} \cdot \dot{\mathbf{u}} \, d\mathcal{B}, \quad (4c)$$

$$\Pi^{ext} = f(\mathbf{u}) = \int_{\mathcal{B}} \hat{\mathbf{b}} \cdot \mathbf{u} \, d\mathcal{B} + \int_{G_s} \hat{\mathbf{t}} \cdot \mathbf{u} \, d\mathcal{B}. \quad (4d)$$

Consider Hamilton’s principle for the problem

$$H(\mathbf{u}) = \int_I \left(T - \Pi^{int} + \Pi^{ext} \right) dt \rightarrow \text{stat}, \quad (5a)$$

$$H(\mathbf{u}) = \int_I \left(\frac{1}{2} (\rho \dot{\mathbf{u}}, \dot{\mathbf{u}}) - \frac{1}{2} a(\mathbf{u}, \mathbf{u}) + f(\mathbf{u}) \right) dt \rightarrow \text{stat}. \quad (5b)$$

The Hamilton’s principle imposes relations between velocity, momenta and displacements in strong form

$$\mathbf{v} = \dot{\mathbf{u}} \quad \mathbf{p} = \rho \mathbf{v} \quad \mathbf{p} = \rho \dot{\mathbf{u}}. \quad (6)$$

These conditions enter in (5b) using the penalty method. To construct the penalty term for the kinematic equation $\mathbf{v} - \dot{\mathbf{u}} = 0$, the difference $\mathbf{v} - \dot{\mathbf{u}}$ is squared and weighted with the density ρ and a dimensionless penalty factor $\frac{1}{2} C_3$.

Finally, it is integrated over the domain, resulting in

$$\mathbf{v} - \dot{\mathbf{u}} = 0 \rightarrow (\mathbf{v} - \dot{\mathbf{u}})^2 = 0 \rightarrow \frac{1}{2} C_3 \rho (\mathbf{v} - \dot{\mathbf{u}})^2 = 0 \rightarrow \int_{\mathcal{B}} \frac{1}{2} C_3 \rho (\mathbf{v} - \dot{\mathbf{u}})^2 \, d\mathcal{B} = \frac{1}{2} C_3 (\rho (\dot{\mathbf{u}} - \mathbf{v}), \dot{\mathbf{u}} - \mathbf{v}) = 0 \quad (7)$$

Analogous considerations for two other relations of (6) lead to two terms with penalty factors C_1 and C_2 . Summing up all terms provides a new expression for the kinetic energy

$$T^\circ = \frac{1}{2} (\rho \dot{\mathbf{u}}, \dot{\mathbf{u}}) + \frac{C_1}{2} \left(\rho \dot{\mathbf{u}} - \mathbf{p}, \dot{\mathbf{u}} - \frac{\mathbf{p}}{\rho} \right) + \frac{C_2}{2} \left(\rho \mathbf{v} - \mathbf{p}, \mathbf{v} - \frac{\mathbf{p}}{\rho} \right) + \frac{C_3}{2} (\rho (\dot{\mathbf{u}} - \mathbf{v}), \dot{\mathbf{u}} - \mathbf{v}). \quad (8)$$

The penalized Hamilton’s principle uses T° as

$$H^\circ(\mathbf{u}, \mathbf{v}, \mathbf{p}) = \int_I \left(T^\circ - \Pi^{int} + \Pi^{ext} \right) dt \rightarrow \text{stat.} \quad (9)$$

The first variation of (9) gives

$$\begin{aligned} \delta H^\circ(\mathbf{u}, \mathbf{v}, \mathbf{p}) &= \int_I \left(\delta \mathbf{p}, (C_1 + C_2) \frac{\mathbf{p}}{\rho} - C_1 \dot{\mathbf{u}} - C_2 \mathbf{v} \right) dt \\ &+ \int_I (\delta \mathbf{v}, (C_2 + C_3) \rho \mathbf{v} - C_3 \rho \dot{\mathbf{u}} - C_2 \mathbf{p}) dt \\ &+ \int_I [(\delta \dot{\mathbf{u}}, (1 + C_1 + C_3) \rho \dot{\mathbf{u}} - C_3 \rho \mathbf{v} - C_1 \mathbf{p}) - \delta \Pi] dt \end{aligned} \quad (10)$$

Integrating $(\delta \dot{\mathbf{u}}, (1 + C_1 + C_3) \rho \dot{\mathbf{u}} - C_3 \rho \mathbf{v} - C_1 \mathbf{p})$ by parts in time yields

$$- \int_I \left(\delta \mathbf{u}, \frac{d}{dt} \{ (1 + C_1 + C_3) \rho \dot{\mathbf{u}} - C_3 \rho \mathbf{v} - C_1 \mathbf{p} \} \right) dt \quad (11)$$

Substitution of (11) into (10) gives a weak formulation, proposed herein.

The Euler-Lagrange equations of the weak form (10) compose a system of equations

$$\begin{cases} \frac{d}{dt} \{ (1 + C_1 + C_3) \rho \dot{\mathbf{u}} - C_3 \rho \mathbf{v} - C_1 \mathbf{p} \} \\ = \text{div} \boldsymbol{\sigma} + \hat{\mathbf{b}} & \text{in } I \times \mathcal{B} \\ \boldsymbol{\sigma} \mathbf{n} = \hat{\mathbf{t}} & \text{in } I \times \partial \mathcal{B}_\sigma \\ (C_1 + C_2) \mathbf{p} - C_2 \rho \mathbf{v} = C_1 \rho \dot{\mathbf{u}} & \text{in } I \times \mathcal{B} \\ -C_2 \mathbf{p} + (C_2 + C_3) \rho \mathbf{v} = C_3 \rho \dot{\mathbf{u}} & \text{in } I \times \mathcal{B} \end{cases} \quad (12)$$

Consider the two last equations in (12). They are a system of two linear equations with respect to \mathbf{p} and \mathbf{v} . If the determinant of the coefficient matrix is non-zero, i.e. $C_1 C_2 + C_2 C_3 + C_1 C_3 \neq 0$, then we can solve for \mathbf{p} and \mathbf{v} , leading to

$$\mathbf{v} = \dot{\mathbf{u}} \quad \mathbf{p} = \rho \dot{\mathbf{u}}. \quad (13)$$

Thus, the subsidiary conditions (6) are recovered as Euler-Lagrange equations. Substitution of the latter in the first equation of (12) gives the equation of motion in the form (2₁). This proves the equivalence of the penalized Hamilton’s principle to the IBVP (2–3).

Note, that the form T° is quadratic and symmetric with respect to the triple $[\dot{\mathbf{u}}, \mathbf{v}, \mathbf{p}]$

$$2T^\circ = \int_{\mathcal{B}} \begin{bmatrix} \rho \dot{\mathbf{u}} \\ \rho \mathbf{v} \\ \mathbf{p} \end{bmatrix}^T \begin{bmatrix} 1 + C_1 + C_3 & -C_3 & -C_1 \\ -C_3 & C_2 + C_3 & -C_2 \\ -C_1 & -C_2 & C_2 + C_3 \end{bmatrix} \begin{bmatrix} \dot{\mathbf{u}} \\ \mathbf{v} \\ \mathbf{p} \end{bmatrix} \, d\mathcal{B}. \quad (14)$$

The positive definiteness of the form is verified by Sylvester’s criterion. If leading principal minors of the matrix of the quadratic form are all positive, then the form is positive definite. These conditions reads as follows

$$\begin{cases} C_1 + C_3 > -1 \\ C_2 + C_3 > 0 \\ C_1 C_2 + C_2 C_3 + C_1 C_3 > 0. \end{cases} \quad (15)$$

Thus, the form fulfills the requirement for the new variational formulation given in problem statement.

The formulation (10) can be interpreted as a parametrized (template) variational principle [6]. The formulation contains all canonical variational principles of a linear elastodynamics as particular cases. The standard Hamiltonian’s principle is obtained for $C_1 = C_2 = C_3 = 0$. The modified Hamiltonian’s principle is recovered for $C_1 = -C_2 = -1$ and $C_3 = 0$. The Hellinger-Reissner principle is recovered for $C_1 = C_2 = 0$ and $C_3 = -1$ [7]. This implies completeness of the parametrization. Moreover, the form T° satisfies the consistency conditions for a template stated in [6]. The row sums of the matrix coefficient of the form are one, zero and zero for the first, second and third row, respectively.

4 Discretization

In the previous section a weak formulation for elastodynamics (10) was derived. This formulation has three independent variables $[\mathbf{u}, \mathbf{v}, \mathbf{p}]$ and contains three scalar penalty parameters (C_1, C_2, C_3) . Discretization of the free variables can be written as

$$\mathbf{u}^h = \mathbf{N} \mathbf{U} \quad \mathbf{v}^h = \boldsymbol{\psi} \mathbf{V} \quad \mathbf{p}^h = \boldsymbol{\chi} \mathbf{P} \quad (16a)$$

$$\delta \mathbf{u}^h = \mathbf{N} \delta \mathbf{U} \quad \delta \mathbf{v}^h = \boldsymbol{\psi} \delta \mathbf{V} \quad \delta \mathbf{p}^h = \boldsymbol{\chi} \delta \mathbf{P} \quad (16b)$$

Here, \mathbf{N} contains shape functions for interpolation of nodal displacements, given by the vector \mathbf{U} . Matrices $\boldsymbol{\psi}$ and $\boldsymbol{\chi}$ interpolate velocity and momentum from vectors of parameters \mathbf{V} and \mathbf{P} . In contrast to the displacement vector \mathbf{U} , parameters \mathbf{V} and \mathbf{P} are not necessarily nodal values. Finally, the shape functions for variations are the same as for variables.

Substitution of (16b) in (10) with (11) yields

$$\begin{aligned} \delta H^{o,h}(\mathbf{u}, \mathbf{v}, \mathbf{p}) = & \int_I \delta \mathbf{P} \left(-C_1 \mathbf{C}^T \dot{\mathbf{U}} - C_2 \mathbf{G}^T \mathbf{V} + (C_1 + C_2) \mathbf{G} \mathbf{P} \right) dt \\ & + \int_I \delta \mathbf{V} \left(-C_3 \mathbf{A}^T \dot{\mathbf{U}} + (C_2 + C_3) \mathbf{Y} \mathbf{V} - C_2 \mathbf{G} \mathbf{P} \right) dt \\ & + \int_I \delta \mathbf{U} \left((1 + C_1 + C_3) \mathbf{M} \ddot{\mathbf{U}} - C_3 \mathbf{A} \dot{\mathbf{V}} - C_1 \mathbf{C} \dot{\mathbf{P}} \right) dt \\ & + \int_I \delta \mathbf{U} (\mathbf{K} \mathbf{U} - \mathbf{F}^{\text{ext}}) dt \end{aligned} \quad (17)$$

Here, \mathbf{K} and \mathbf{F}^{ext} are the stiffness matrix and the vector of external forces. Furthermore, we define the following matrices

$$\begin{aligned} \mathbf{M} &= \int_{\mathcal{B}} \rho \mathbf{N}^T \mathbf{N} d\mathcal{B} & \mathbf{A} &= \int_{\mathcal{B}} \rho \mathbf{N}^T \boldsymbol{\psi} d\mathcal{B} \\ \mathbf{C} &= \int_{\mathcal{B}} \mathbf{N}^T \boldsymbol{\chi} d\mathcal{B} & \mathbf{Y} &= \int_{\mathcal{B}} \rho \boldsymbol{\psi}^T \boldsymbol{\psi} d\mathcal{B} \\ \mathbf{G} &= \int_{\mathcal{B}} \boldsymbol{\psi}^T \boldsymbol{\chi} d\mathcal{B} & \mathbf{H} &= \int_{\mathcal{B}} \rho^{-1} \boldsymbol{\chi}^T \boldsymbol{\chi} d\mathcal{B} \end{aligned} \quad (18)$$

\mathbf{M} is the CMM.

Using independence of the variations $\delta \mathbf{U}$, $\delta \mathbf{V}$ and $\delta \mathbf{P}$, we obtain the following system of equations

$$\begin{cases} (1 + C_1 + C_3) \mathbf{M} \ddot{\mathbf{U}} - C_3 \mathbf{A} \dot{\mathbf{V}} - C_1 \mathbf{C} \dot{\mathbf{P}} + \mathbf{K} \mathbf{U} = \mathbf{F}^{\text{ext}} \\ (C_2 + C_3) \mathbf{Y} \mathbf{V} - C_2 \mathbf{G} \mathbf{P} = C_3 \mathbf{A}^T \dot{\mathbf{U}} \\ -C_2 \mathbf{G}^T \mathbf{V} + (C_1 + C_2) \mathbf{H} \mathbf{P} = C_1 \mathbf{C}^T \dot{\mathbf{U}} \end{cases} \quad (19)$$

The variables \mathbf{V} and \mathbf{P} can be eliminated from the equation (19) yielding equations of motion

$$\mathbf{M}^o \ddot{\mathbf{U}} + \mathbf{K} \mathbf{U} = \mathbf{F}^{\text{ext}}, \quad (20)$$

with the scaled mass matrix being $\mathbf{M}^o = \mathbf{M} + \lambda^o$. The artificially added mass λ^o is given by an expression

$$\begin{aligned} \lambda^o &= (C_1 + C_3) \mathbf{M} \\ &- \begin{bmatrix} C_3 \mathbf{A} \\ C_1 \mathbf{C} \end{bmatrix} \begin{bmatrix} (C_2 + C_3) \mathbf{Y} & -C_2 \mathbf{G} \\ C_2 \mathbf{G}^T & (C_1 + C_2) \mathbf{H} \end{bmatrix}^{-1} \begin{bmatrix} C_3 \mathbf{A}^T \\ C_1 \mathbf{C}^T \end{bmatrix} \\ &= (C_1 + C_3) \mathbf{M} - \frac{C_3^2}{C_2 + C_3} \mathbf{A}^T \mathbf{Y}^{-1} \mathbf{A} \\ &+ \frac{C_2^2 C_3}{(C_2 + C_3)^2} \mathbf{A}^T \mathbf{Y}^{-1} \mathbf{G} \mathbf{S} \mathbf{G}^T \mathbf{Y}^{-1} \mathbf{A} + C_1^2 \mathbf{C} \mathbf{S} \mathbf{C}^T \\ &- \frac{C_1 C_2 C_3}{C_2 + C_3} \left(\mathbf{A} \mathbf{Y}^{-1} \mathbf{G} \mathbf{S} \mathbf{C}^T + \mathbf{C} \mathbf{S} \mathbf{G}^T \mathbf{Y}^{-1} \mathbf{A}^T \right). \end{aligned} \quad (21)$$

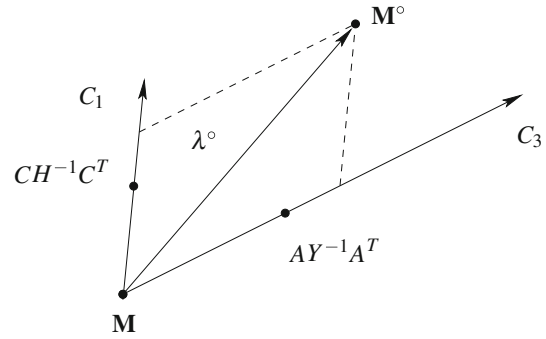


Fig. 1 Linear family of mass matrices \mathbf{M}^o with added mass λ^o after (24)

with \mathbf{S} defined as

$$\mathbf{S} = \left((C_1 + C_2) \mathbf{H} - \frac{C_2^2}{C_2 + C_3} \mathbf{G}^T \mathbf{Y}^{-1} \mathbf{G} \right)^{-1}. \quad (22)$$

Formula (21) provides us with the most general expression for a three-parametric family of mass matrices. Actually, the artificial added mass λ^o entering (20) is a rational function of parameters (C_1, C_2, C_3) . It is not practical to use expression (21) directly, because of unclear influence of the individual parameters on the mass matrix. Here, we discuss three cases where the expression (21) substantially simplifies.

4.1 Case 1

Let us set $C_1 = -C_2$ and $C_3 = 0$. In this case the mass matrix λ^o is

$$\lambda^o = C_1 \left(\mathbf{M} - \mathbf{C} \left(\mathbf{G}^T \mathbf{Y}^{-1} \mathbf{G} \right)^{-1} \mathbf{C}^T \right). \quad (23)$$

4.2 Case 2

Let us set $C_2 = 0$. In this case the mass matrix λ^o is

$$\lambda^o = C_1 \left(\mathbf{M} - \mathbf{C} \mathbf{H}^{-1} \mathbf{C}^T \right) + C_3 \left(\mathbf{M} - \mathbf{A} \mathbf{Y}^{-1} \mathbf{A}^T \right). \quad (24)$$

4.3 Case 3

Let us set $C_1 = C_2 = 0$. In this case the mass matrix λ^o is

$$\lambda^o = C_3 \left(\mathbf{M} - \mathbf{A} \mathbf{Y}^{-1} \mathbf{A}^T \right). \quad (25)$$

In all the cases we obtain linear families of mass matrices, which clarifies the meaning of penalty parameters C_1 and C_3 as scaling factors for artificially added mass, see Fig. 1. The matrices $\mathbf{A} \mathbf{Y}^{-1} \mathbf{A}^T$, $\mathbf{C} \mathbf{H}^{-1} \mathbf{C}^T$ and $\mathbf{C} \left(\mathbf{G}^T \mathbf{Y}^{-1} \mathbf{G} \right)^{-1} \mathbf{C}^T$ are consistent hybrid-mixed mass matrices computed on mixed Hamilton’s principle with variables $[\dot{\mathbf{u}}, \mathbf{v}]$, $[\dot{\mathbf{u}}, \mathbf{p}]$ and $[\dot{\mathbf{u}}, \mathbf{v}, \mathbf{p}]$, respectively. Such mass matrices were defined, e.g. in [8]. Thus, the proposed families (23–25) are weighted

sums of known consistent mass matrices and the proposed variational formulation (10) justifies such a construction. In addition, positive definiteness of \mathbf{M}° is guaranteed if penalty parameters C_1 and C_3 are positive. The structure of λ° given in (23–25) explains the way the proposed mass scaling works. The CMM and hybrid-mixed mass matrices are equal if the ansatz space for \mathbf{v} and \mathbf{p} are taken equal to \mathbf{u} . This results in zero λ° . If the ansatz space for \mathbf{v} and \mathbf{p} are chosen poorer than for \mathbf{u} , the hybrid-mixed mass matrices produce less inertia than a CMM. Thus, the artificially added mass increases inertia for modes orthogonal to the ansatz space for \mathbf{v} and \mathbf{p} . The appropriate ansatz spaces are discussed in subsequent subsections.

4.4 Example: 3-node membrane element

A simple example is discussed to clarify the approach. Consider a 3-node membrane element with constant density ρ . Let us stick to the case with $C_2 = C_3 = 0$, leading to $\mathbf{M}^\circ = \mathbf{M} + C_1(\mathbf{M} - \mathbf{C}\mathbf{H}^{-1}\mathbf{C}^T)$. We use standard shape functions for displacements and constant functions for momenta

$$\mathbf{N} = \begin{bmatrix} 1 - \xi - \eta & 0 & \xi & 0 & \eta & 0 \\ 0 & 1 - \xi - \eta & 0 & \xi & 0 & \eta \end{bmatrix}, \mathbf{X} = \begin{bmatrix} 1 & 0 \\ 0 & 1 \end{bmatrix} \quad (26)$$

Substitution of the latter leads to

$$\mathbf{M} = \frac{\rho A_0}{12} \begin{bmatrix} 2 & 0 & 1 & 0 & 1 & 0 \\ 0 & 2 & 0 & 1 & 0 & 1 \\ 1 & 0 & 2 & 0 & 1 & 0 \\ 0 & 1 & 0 & 2 & 0 & 1 \\ 1 & 0 & 1 & 0 & 2 & 0 \\ 0 & 1 & 0 & 1 & 0 & 2 \end{bmatrix}, \mathbf{C}^T = \frac{A_0}{3} \begin{bmatrix} 1 & 0 \\ 0 & 1 \\ 1 & 0 \\ 0 & 1 \\ 1 & 0 \\ 0 & 1 \end{bmatrix}, \quad (27)$$

$$\mathbf{H} = \frac{A_0}{\rho} \begin{bmatrix} 1 & 0 \\ 0 & 1 \end{bmatrix},$$

$$\lambda^\circ = C_1 \frac{\rho A_0}{18} \begin{bmatrix} 2 & 0 & -1 & 0 & -1 & 0 \\ 0 & 2 & 0 & -1 & 0 & -1 \\ -1 & 0 & 2 & 0 & -1 & 0 \\ 0 & -1 & 0 & 2 & 0 & -1 \\ -1 & 0 & -1 & 0 & 2 & 0 \\ 0 & -1 & 0 & -1 & 0 & 2 \end{bmatrix}. \quad (28)$$

The latter expression is identical up to a factor to the mass scaling matrix λ presented in [3]. To obtain mass scaling identical to [3] for a 8-node solid brick element (brick), one should take as \mathbf{M} in (21) a lumped matrix and $\mathbf{X} = \frac{J_0}{J} \mathbf{I}_{3 \times 3}$ with J and J_0 being the Jacobian and the Jacobian in the center of the element, $\mathbf{I}_{3 \times 3}$ being the identity matrix.

5 Good ansatz spaces for mass scaling

Justification of existing methods is not the only goal of this paper. Flexibility of the mass matrices (23–25) facilitates construction of SMS that does not have some of the disadvantages of existing techniques. For example, some mass scaling technique do not preserve rotational inertia of a single element. This leads to large errors for problems where substantial rotations of a structure occurs. If the ansatz space for velocities contains all rigid body modes (RBM), then mass matrix (25) gives the exact values for translational and rotational inertia. For 2D and 3D cases following ψ is required

$$\psi_{2D} = \begin{bmatrix} 1 & 0 & -y^h \\ 0 & 1 & x^h \end{bmatrix}, \psi_{3D} = \begin{bmatrix} 1 & 0 & 0 & -y^h & z^h & 0 \\ 0 & 1 & 0 & x^h & 0 & -z^h \\ 0 & 0 & 1 & 0 & -x^h & y^h \end{bmatrix}. \quad (29)$$

Here, $x^h(\xi, \eta, \zeta)$, $y^h(\xi, \eta, \zeta)$ and $z^h(\xi, \eta, \zeta)$ are approximations of element geometry obtained from the isoparametric approach. However, such velocity shape functions ψ lead to a mass matrix \mathbf{M}° with coupled terms between x -, y - and z - direction. This is a rather undesired property both from numerical and physical view. The coupled terms increase fill-in of the mass matrix, raise the cost of each individual step of iterative solution for the accelerations and negatively affect conditioning of the mass matrix. In order to decouple inertia, each column of ψ should contain only one non-zero entry. This leads to a different ansatz ψ

$$\psi_{2D} = \begin{bmatrix} 1 & 0 & y^h & 0 \\ 0 & 1 & 0 & x^h \end{bmatrix},$$

$$\psi_{3D} = \begin{bmatrix} 1 & 0 & 0 & y^h & z^h & 0 & 0 & 0 & 0 \\ 0 & 1 & 0 & 0 & 0 & 0 & x^h & 0 & z^h \\ 0 & 0 & 1 & 0 & 0 & x^h & 0 & y^h & 0 \end{bmatrix}. \quad (30)$$

Furthermore, we use as a reference ψ with only constant terms

$$\psi_{2D} = \begin{bmatrix} 1 & 0 \\ 0 & 1 \end{bmatrix}, \psi_{3D} = \begin{bmatrix} 1 & 0 & 0 \\ 0 & 1 & 0 \\ 0 & 0 & 1 \end{bmatrix}. \quad (31)$$

In the following section, some examples demonstrate the efficiency of the proposed techniques.

6 Examples

The proposed family of mass matrices is obtained from novel variational formulations and it is tested in three examples. In the first and the second example the influence of the proposed mass scaling techniques on eigenvalues of structures is studied. These problems are small enough so that the full spectra can be obtained and analyzed. Efficiency of mass scaling is estimated by the reduction of maximum frequency ω_{max} . The spectrum computed for a LMM is taken as a reference.

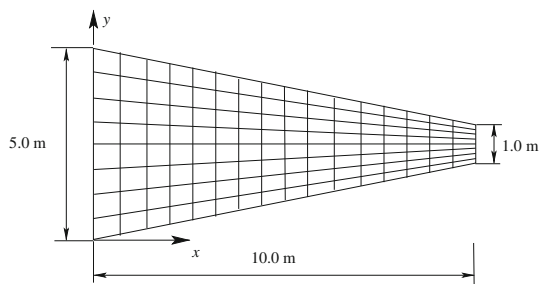


Fig. 2 Setup of FV32 NAFEMS benchmark. Material properties: $E = 200$ GPa, $\nu = 0.3$, $\rho = 8,000$ kg/m³. Thickness: 0.05 m. Mesh: 16×8 elements

Additionally, we check the condition number of mass matrices and the maximum error in lowest 10% range of spectra, which is important for the structural response.

In the third example we compare efficiency and accuracy of mass scaling for a transient problem taken from [3]. A central difference time integration scheme is used. The critical time step for different mass matrices is estimated with power iterations [9]. For each mass matrix a time step being 0.63 of a critical time step is used. Efficiency of mass scaling is estimated by the number of required time steps. Accuracy is checked against solution obtained for a LMM.

6.1 Cantilevered tapered membrane: FV32

As an example of a two-dimensional problem, the eigenfrequency benchmark FV32 of NAFEMS [10] is considered. Geometry, mesh and material properties of the model are presented in Fig. 2. Boundary conditions $u_x = u_y = 0$ are imposed along the y -axis. Bilinear 4-node elements with four enhanced strains are used for stiffness calculation. In Fig. 3, we show the reduction of eigenfrequencies for different values of the scaling parameter C_1 for ansatz (29). Increase of C_1 decreases the maximum frequency. For $C_1 < 5$ the maximum frequency of the scaled mass matrix is higher than for the LMM. For $C_1 = 20$ the maximum frequency is halved and for $C_1 = 30$ decreased by a factor of three. Comparable reduction of maximum frequency can be obtained for method from [3] with $\beta = 2$, however the error in lowest eigenfrequencies for the proposed method is less. In Table 1 we examine performance of the proposed method for a set of ansatz function for velocity ψ with fixed penalty value $C_1 = 30$. For the reference, performance of the method II [3] is also given.

6.2 Simply supported square plate: FV52

As an example of a three-dimensional problem, the eigenfrequency benchmark FV52 of NAFEMS [10] is considered. Geometry and mesh of the model are shown in Fig. 4. Material properties of the benchmark FV52 are identical to FV32.

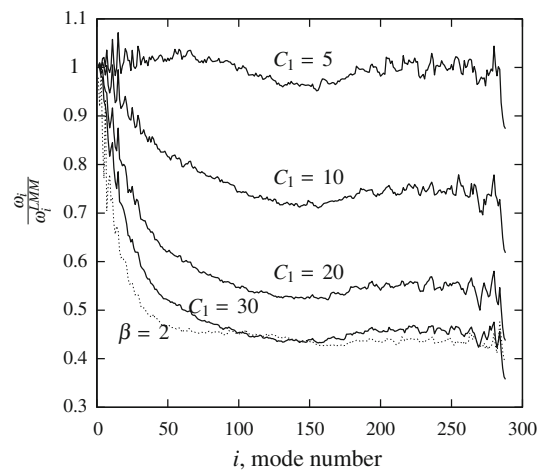


Fig. 3 Ratio of eigenfrequencies for different values of selective mass scaling parameters. C_1 —proposed in paper with ψ from (29), β —method II [3]

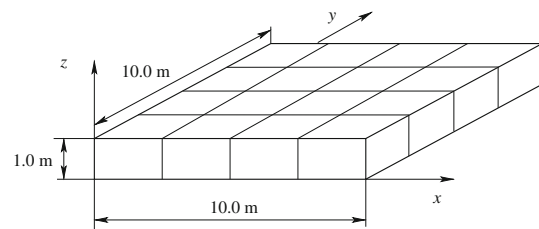


Fig. 4 Geometry and mesh of FV52 NAFEMS benchmark. Material properties: $E = 200$ GPa, $\nu = 0.3$, $\rho = 8,000$ kg/m³. Mesh: $8 \times 8 \times 1$ elements

Boundary conditions $u_z = 0$ are imposed along all four lower edges ($z = -0.5$). For stiffness calculation 8-node solid elements with nine enhanced strains are used. SMS is computed with ansatz after (29). The reductions of eigenfrequencies obtained for different values of scaling parameter are shown in Fig. 5. The reduction of 40, 55 and 65% is obtained for $C_1 = 10, 20$ and 30 , respectively. The accuracy of the lowest eigenfrequencies is compared with method from [3]. For $\beta = 2$ the error in lowest 10% range of eigenfrequencies is 40% against the error 13% for $C_1 = 10$.

6.3 Tip loaded cantilever beam

The model for a transient problem is shown in Fig. 6. Initial zero displacements and velocities are assumed. The beam is loaded at the tip by an abrupt force F . Structural response is compared using the history of the tip displacement w , Fig. 7. The deflections obtained with a LMM and the proposed SMS are almost identical even for high value of scaling. For the same reduction of time steps, the method [3] yield a bigger error.

Computation with a regular LMM required 12,900 time steps. For the number of time steps for different mass

Table 1 Comparison of different mass scaling formulations for FV32, $C_1 = 30$

ψ from	(29)	(30)	(31)	After [3], $\beta = 2$
ω_{max} , Hz	4,045	7,198	4,036	4,459
$\omega_{max}/\omega_{max}^{LMM}$	0.35	0.63	0.35	0.39
Cond (\mathbf{M})	26.9	39.3	14.1	11.0
Error in lowest 10% freq., %	38	31	56	49

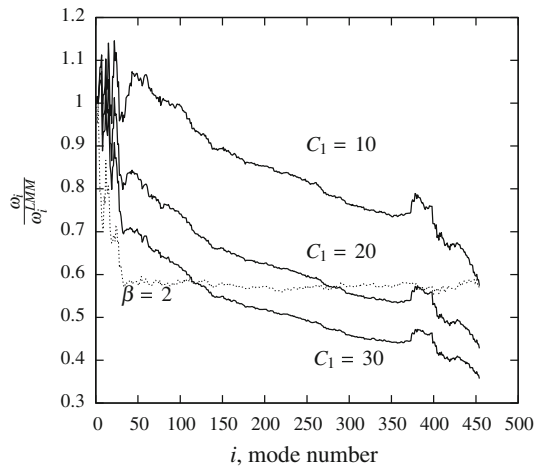


Fig. 5 Ratio of eigenfrequencies for different values of selective mass scaling parameters. C_1 —proposed in paper with ψ from (29), β —method II [3]

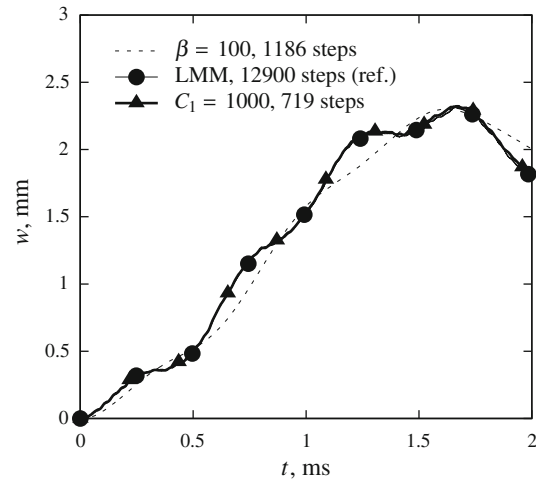


Fig. 7 Tip deflection w of a cantilever beam

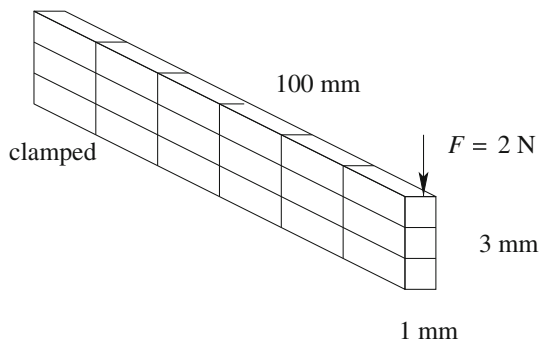


Fig. 6 The model of tip loaded beam [3]. Material properties: $E = 207$ GPa, $\nu = 0.0$, $\rho = 7,800$ kg/m³. Mesh: $50 \times 3 \times 1$ elements

matrices the following results are obtained. The CMM requires 21,106 time steps, which is almost twice that of LMM. The proposed method adds inertia to the CMM (25), therefore after mass scaling the required number of time steps is always less than the number. Application of the ansatz ψ from (30) does not decrease time step substantially. It is even more than 12,900 that is obtained for the LMM, therein ansatz (30) is not pursued further. The reason for such a poor behavior is inability of this ansatz to decrease volumetric modes. The ansatz contains full linear subspace of velocities, i.e. a constant volumetric strain rate. The mesh of the example uses

one element through the thickness and the volumetric modes are not constrained by neighboring elements. (31) and (29) give comparable reduction of number of steps, e.g. 2,248 and 2,392 for $C_1 = 100$, 717 and 719 for $C_1 = 1,000$, respectively. For comparison, mass scaling with $\beta = 100$ from [3] cuts down number of steps to 1,186.

The accuracy of SMS can be monitored by the kinetic energy stored in artificially added mass $T^\circ - T = \frac{1}{2} \dot{\mathbf{u}} \lambda^\circ \dot{\mathbf{u}}$. The small ratio of the artificially added kinetic energy to the total energy indicate little change in structural response. For the problem at hand, the ratio of that artificial energy to the total energy is presented in Fig. 8. From the Figure is clear that the proposed method accumulates much less artificially added energy than the method proposed in [3].

During numerical experiments a negative feature of (29) and (30) was found. The number of iterations for the solution of $\ddot{\mathbf{u}} = \mathbf{M}^{-1} \mathbf{f}$ was two to three times larger compared to (31) and [3]. Moreover, the iterative solver diverged for $C_1 > 100$ and a direct sparse solver was used instead. Both SMS matrices from (29) to (30) result in a bigger fill-in of the mass matrix and worse conditioning number in comparison to (31) and [3]. So far it is not clear which of these two features is the key for worse convergence of an iterative solver. This issue requires further studies.

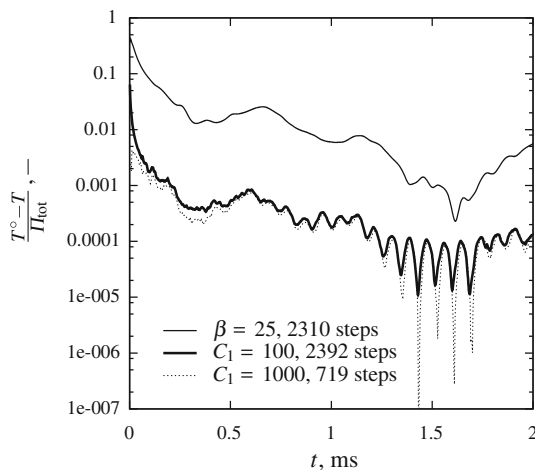


Fig. 8 Ratio of kinetic energy stored in artificially added mass to total energy

7 Conclusions

A new variational method for SMS has been presented. We propose to use a new penalized Hamilton's principle as starting point of discretization. Together with appropriate ansatz spaces for velocity and momentum, the proposed approach results in parametric families of *consistent* mass matrices. Usage of these mass matrices decreases the maximum eigenfrequency of the system and increases the critical time step. At the same time the lowest eigenfrequencies in the range of interest and structural response are not significantly changed.

The main theoretical result of this work is the new parametric principle for elasto-dynamics. It is a modification of Hamilton's principle where kinematic and kinetic equations are satisfied via a penalty method. Its discretization yields a general expression of a mass matrix. We choose three sub-families that are efficient for numerical implementation.

It is also shown that the mass scaling technique presented in [3] can be obtained as a special case of the present formulation and thus it is variationally justified. The main practical result is a study of several instances of proposed mass scaling. Ansatz spaces for velocity are constructed that preserve rotational inertia. The numerical examples show that the best results are obtained with a formulation with the velocity field just containing the rigid body modes. This formulation also outperforms the method presented in [3] in the investigated examples.

Computation of problem with large rotations and with a variable mass matrix is a possible extension of the work. The shape functions ψ from (29) are time dependent and artificial added mass is changing in time λ° . This yields an additional term in the equilibrium equation $\dot{\mathbf{U}}$. Such a term may be significant for large mass scaling factors, otherwise it can be neglected. Computation of $\frac{\partial \lambda^\circ}{\partial t}$ is not complicated. The treatment of a similar term is explained, e.g. in [11, p. 523]. It is also desirable to study the influence of SMS on eigenmodes and the sensitivity of SMS to mesh distortions [5], which has not been done in the present work.

Acknowledgments Support of Baden-Württemberg Stiftung gGmbH Grant HPC-10 and Deutsche Forschungsgemeinschaft Grant BI 722_7.1 is gratefully acknowledged.

References

- Olovsson L, Simonsson K (2006) Iterative solution technique in selective mass scaling. *Commun Numer Methods Eng* 22(1):77–82. doi:10.1002/cnm.806
- Olovsson L, Unosson M, Simonsson K (2004) Selective mass scaling for thin walled structures modeled with tri-linear solid elements. *Comput Mech* 34:134–136. doi:10.1007/s00466-004-0560-6
- Olovsson L, Simonsson K, Unosson M (2005) Selective mass scaling for explicit finite element analyses. *Int J Numer Methods Eng* 63(10):1436–1445. doi:10.1002/nme.1293
- Askes H, Nguyen D, Tyas A (2011) Increasing the critical time step: micro-inertia, inertia penalties and mass scaling. *Comput Mech* 47:657–667. doi:10.1007/s00466-010-0568-z
- Cocchetti G, Pagani M, Perego U (2012) Selective mass scaling and critical time-step estimate for explicit dynamic analyses with solid-shell elements. *Comput Struct*. doi:10.1016/J.compstruc.2012.10.021
- Felippa CA (1994) A survey of parametrized variational principles and applications to computational mechanics. *Comput Methods Appl Mech Eng* 113(12):109–139. doi:10.1016/0045-7825(94)90214-3
- Washizu K (1982) *Variational methods in elasticity and plasticity*, 3rd edn. Pergamon Press, Oxford
- Hughes T, Hilber H, Taylor R (1976) A reduction scheme for problems of structural dynamics. *Int J Solids Struct* 12(11):749–767. doi:10.1016/0020-7683(76)90040-8
- Benson D, Bazilevs Y, Hsu M, Hughes T (2010) Isogeometric shell analysis: the reissner-mindlin shell. *Comput Methods Appl Mech Eng* 199(58):276–289. doi:10.1016/j.cma.2009.05.011
- National Agency for Finite Element Methods & Standards (Great Britain) (1990) *The standard NAFEMS benchmarks*. NAFEMS, Orlando
- Belytschko T, Liu W, Moran B (2000) *Nonlinear finite elements for continua and structures*. Wiley, New York